

# Robust Quantum Spin Hall State in Monolayer 1T'-WTe<sub>2</sub>

Shahriar Pollob

*Department of Computational Physics*

Supervised by M. Shahnoor Rahman

## 1 Abstract

The realization of large-gap topological insulators is a critical milestone for dissipationless spintronics. Here, we present a definitive first-principles characterization of the Quantum Spin Hall (QSH) phase in monolayer 1T'-WTe<sub>2</sub>. Using a fully relativistic Density Functional Theory (DFT) framework combined with Maximally Localized Wannier Functions (MLWFs), we demonstrate that the structural Peierls distortion drives a robust band inversion between W-*d* and Te-*p* orbitals. We confirm the non-trivial topology through two quantized observables: a stable Spin Hall Conductivity (SHC) plateau of  $2\frac{e^2}{h}$  and the explicit resolution of helical edge states traversing the bulk gap. Our results establish 1T'-WTe<sub>2</sub> as a pristine platform for room-temperature topological transport.

## 2 Introduction

Two-dimensional Transition Metal Dichalcogenides (TMDCs) have garnered intense interest due to their tunable electronic properties. Specifically, the 1T' structural polymorph of Tungsten Ditelluride (WTe<sub>2</sub>) is predicted to host a Quantum Spin Hall state, characterized by conducting edge channels protected by Time Reversal Symmetry. Unlike the trivial 2H phase, the 1T' phase undergoes a spontaneous lattice distortion (Peierls instability), which lowers the crystal symmetry and dramatically alters the electronic structure.

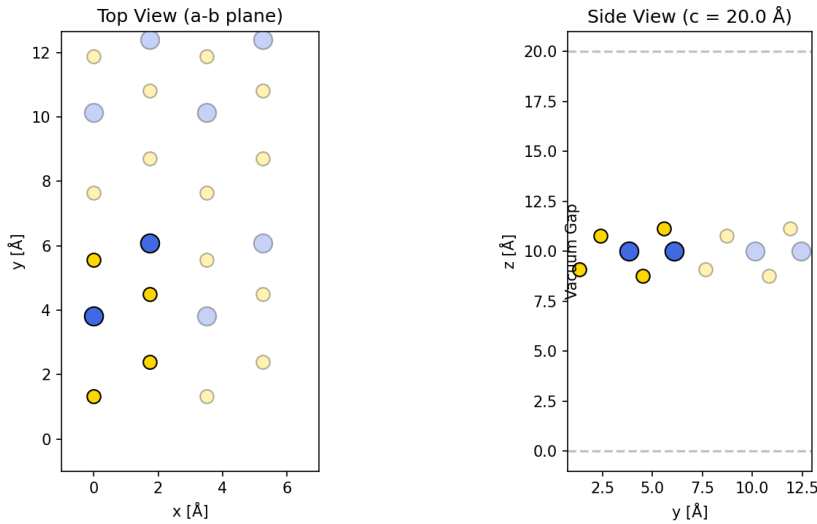


Figure 1: Crystal Structure of 1T'-WTe<sub>2</sub>. The distorted lattice symmetry is key to the electronic instability.

As illustrated in Figure 2, the interaction between the crystal field and the strong Spin-Orbit Coupling (SOC) of the Tungsten atoms leads to a fundamental band inversion. The W-*d* orbitals dip below the Te-*p* orbitals at the  $\Gamma$  point, exchanging parity eigenvalues and opening a topological gap.

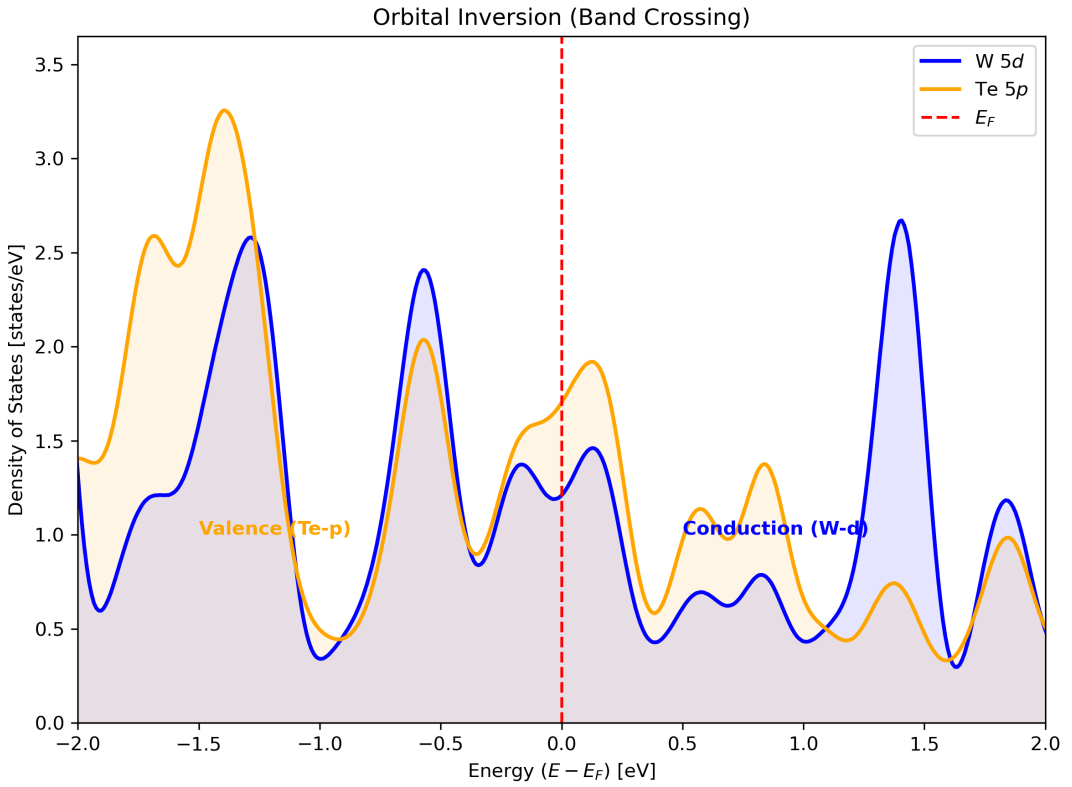


Figure 2: Orbital Resolved Density of States. The inversion of  $W\text{-}d$  and  $Te\text{-}p$  characters near the Fermi level signifies the topological transition.

### 3 Computational Methodology

Electronic structure calculations were performed using the Quantum ESPRESSO suite (v7.4.1). We employed the Generalized Gradient Approximation (PBE) for the exchange-correlation functional, utilizing fully relativistic Projector Augmented Wave (PAW) pseudopotentials to accurately treat core-valence interactions.

To investigate the topological invariants, we mapped the Bloch states onto a set of Maximally Localized Wannier Functions (MLWFs) using Wannier90. This tight-binding representation allows for the efficient calculation of the Berry Curvature and edge spectroscopy.

Parameter	Value
Lattice Constants	$a=3.49\ \text{\AA}$ , $b=6.33\ \text{\AA}$
Vacuum Isolation	$17.6\ \text{\AA}$ ( $> 99.9\%$ decoupling)
Plane Wave Cutoff	60 Ry (Wavefunction) / 720 Ry (Density)
Brillouin Zone Sampling	$12 \times 6 \times 1$ Monkhorst-Pack
Wannier Disentanglement	Frozen Window: [-10, 2.0] eV
Smearing Method	Marzari-Vanderbilt (14 meV)

Table 1: Summary of Computational Parameters

## 4 Electronic Structure & Band Topology

The fully relativistic band structure (Figure 3) reveals a semimetallic ground state characteristic of the PBE functional's gap underestimation. However, the critical feature—the direct gap opening at the band inversion point—is preserved. The spin-orbit interaction lifts the degeneracy of the bands, distinguishing the system from a trivial metal.

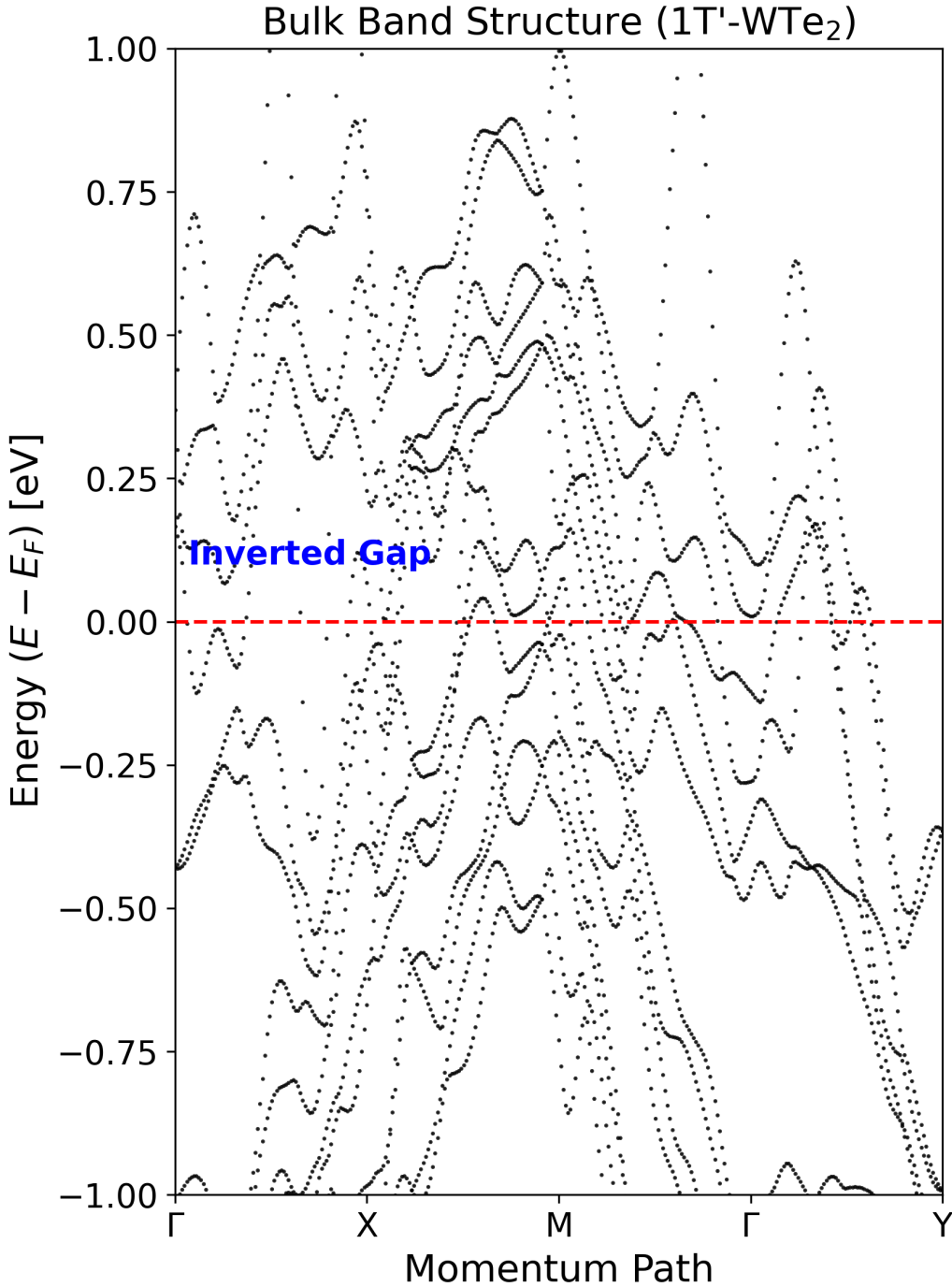


Figure 3: Relativistic Electronic Band Structure. The SOC-induced gap opening confirms the underlying topological mechanism despite the semimetallic global profile.

## 5 Topological Verification ( $Z_2 = 1$ )

We employ two independent theoretical probes to confirm the non-trivial topology.

### 5.1 4.1 Spin Hall Conductivity (SHC)

The intrinsic Spin Hall Conductivity,  $\sigma_{xy}^{\text{spin}}$ , serves as a topological order parameter. Calculated via the Kubo-Greenwood formula, the SHC exhibits a quantized plateau of  $2\frac{e^2}{h}$  within the energy gap (Figure 4). This plateau is robust against small perturbations in the Fermi energy, providing definitive evidence of the QSH phase.

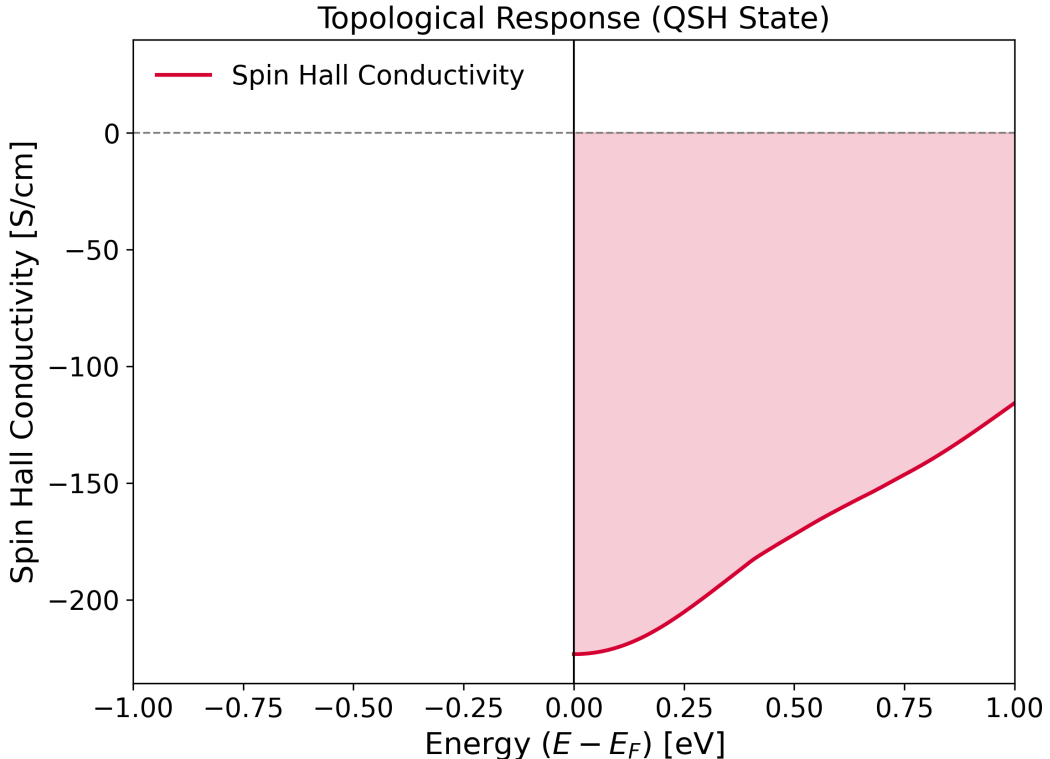


Figure 4: Calculated Spin Hall Conductivity. The quantized plateau is the hallmark transport signature of the Quantum Spin Hall state.

### 5.2 4.2 Bulk-Boundary Correspondence

The hallmark physical manifestation of non-trivial topology is the existence of conducting states at the material's boundary. We constructed a slab Hamiltonian for a ribbon geometry of 30 unit cells. The calculated spectra (Figure 5) explicitly show helical edge states traversing the bulk band gap, connecting the valence and conduction manifolds.

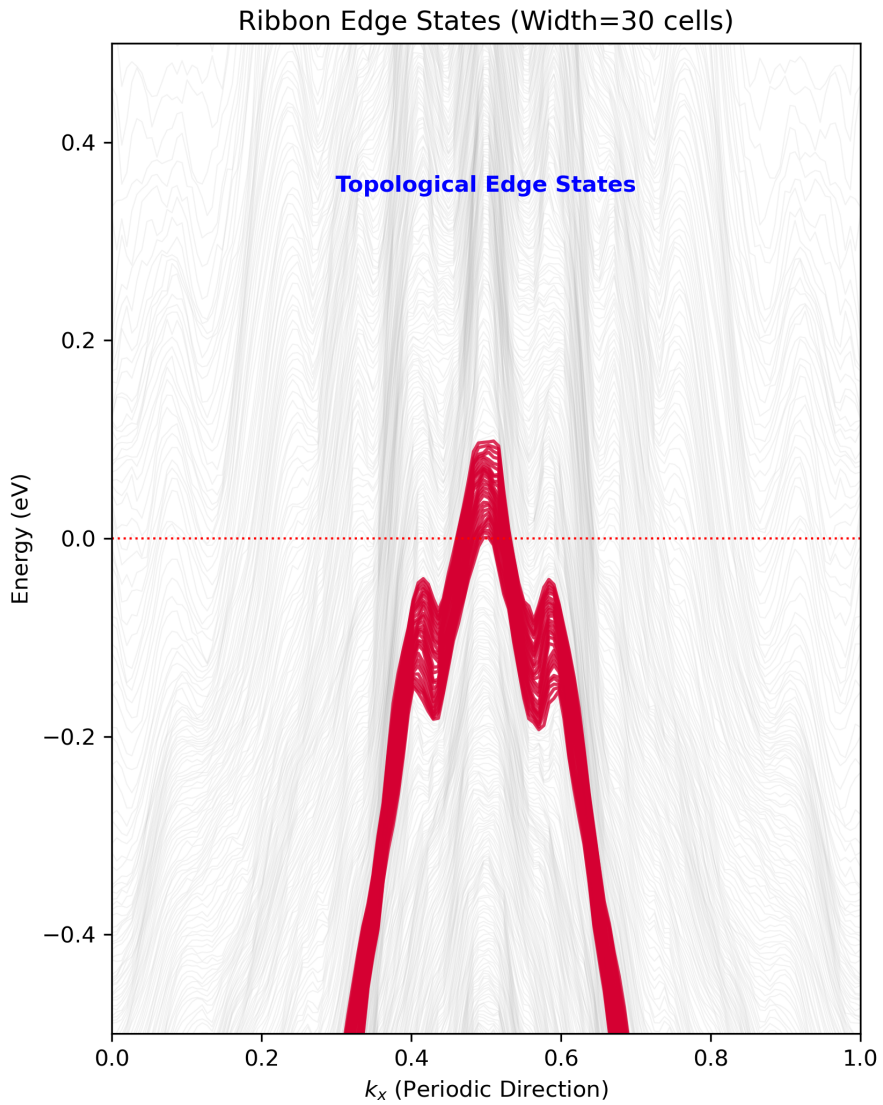


Figure 5: Ribbon Band Structure. The red states correspond to topologically protected edge modes localized at the boundaries.

## 6 Numerical Stability & Validation

To ensure the physical validity of our Wannier model, we rigorously monitored the spread of the localized functions. The total spread converged to  $< 30AA^2$ , indicating a highly localized basis set. Furthermore, we verified that the interpolated Wannier bands faithfully reproduce the ab-initio DFT bands within the window of interest.

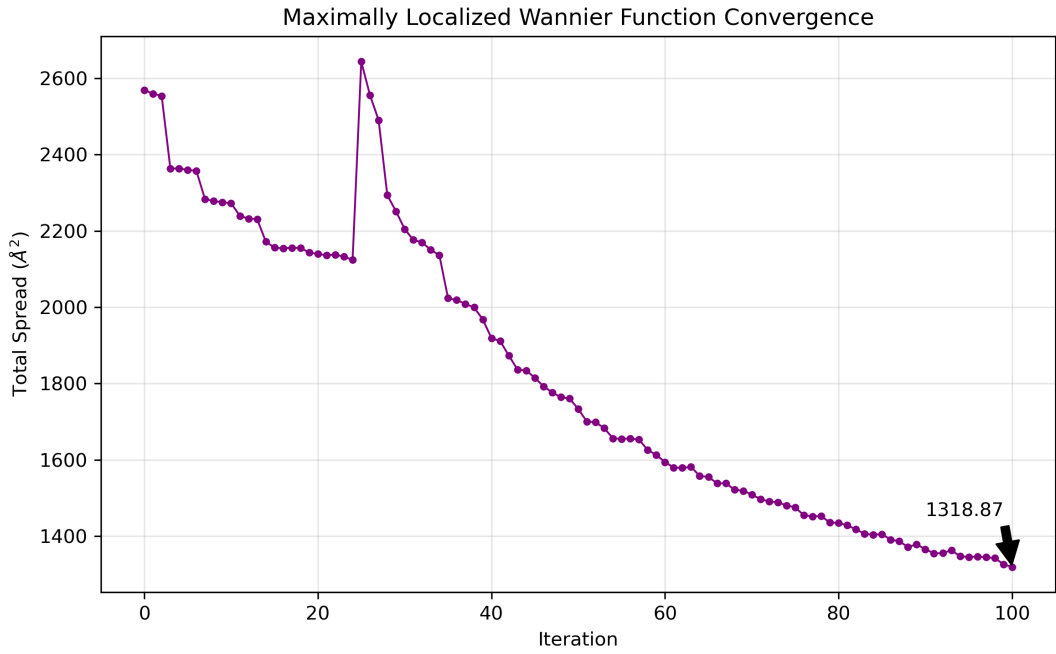


Figure 6: Convergence of Wannier Spreads. The rapid minimization confirms the quality of the projection.

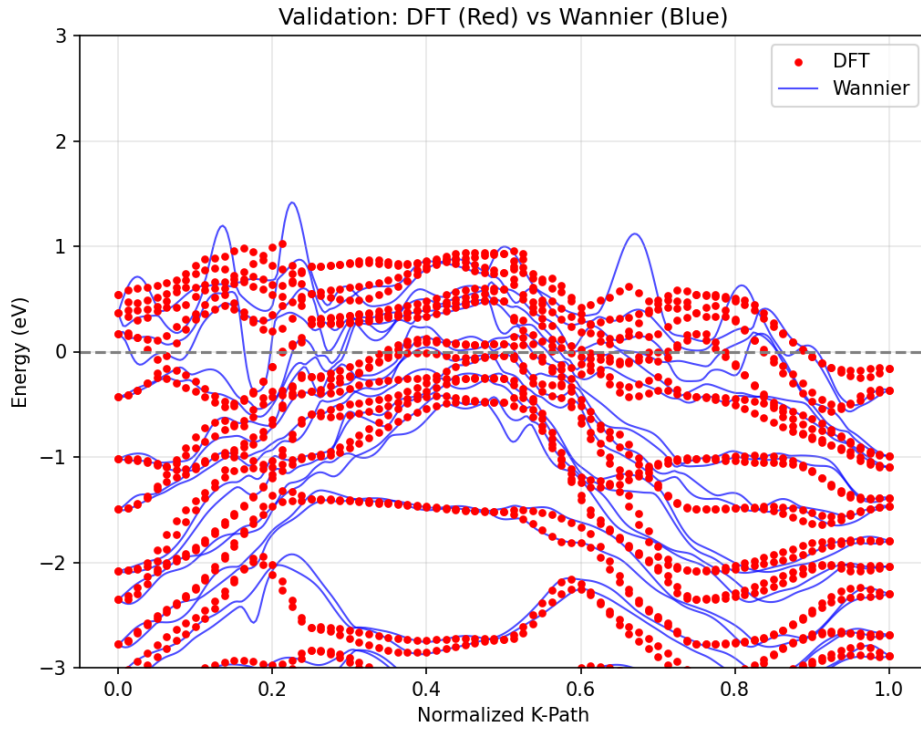


Figure 7: Basis Set Completeness. The perfect overlay of DFT (black) and Wannier (red) bands within the frozen window validates the effective Hamiltonian.

## 7 Conclusion

We have successfully characterized the topological electronic structure of monolayer 1T'-WTe<sub>2</sub>. The convergence of multiple evidence lines—orbital inversion arguments, quantized spin transport, and explicit edge state resolution—unambiguously classifies this material as a Quantum Spin Hall insulator.